MAGNETIC RECONNECTION SCENARIO OF THE BASTILLE DAY 2000 FLARE

BORIS V. SOMOV,[1] TAKEO KOSUGI, HUGH S. HUDSON, AND TARO SAKAO

Institute of Space and Astronautical Science, 3-1-1 Yoshinodai, Sagamihara, Kanagawa 229-8510, Japan

AND

SATOSHI MASUDA

Solar-Terrestrial Environment Laboratory, Nagoya University, 3-13 Honohara, Toyokawa, Aichi 442-8507, Japan

ABSTRACT

On the basis of *Yohkoh* Hard X-Ray Telescope data and the magnetograms taken by the *SOHO* Michelson Doppler Imager and the Solar Magnetic Field Telescope at Huairou Solar Observing Station, we suggest an interpretation of the well-observed " Bastille Day 2000 " flare. The large-scale structure and dynamics of the flare, as seen in hard X-rays, can be explained in terms of the three-dimensional reconnection at a separator in the corona. More specifically, we suggest that before occurrence of two-ribbon flares with significant decrease of a distance between the hard X-ray (HXR) footpoints, like the Bastille Day flare, the bases of magnetic field separatrices are moved by the large-scale photospheric flows of two types. First, the shear flows, which are parallel to the photospheric neutral line, increase the length of field lines in the corona and produce an excess of magnetic energy. Second, the converging flows, i.e., the flows directed to the neutral line, create the preflare current layers in the corona and provide an excess of energy sufficient to produce a large flare. During the flare, both excesses of magnetic energy are released completely or partially. In the Bastille Day flare, the model describes two kinds of apparent motions of the HXR kernels. One is an increase of a distance between the flare ribbons in which the HXR kernels appear. The effect results from fast reconnection in a coronal current layer. The second effect is a decrease of the distance between the kernels moving to each other as a result of relaxation of magnetic tensions generated by the photospheric shear flows.

Subject headings: acceleration of particles — Sun: flares — Sun: magnetic fields — Sun: X-rays, gamma rays

1. INTRODUCTION

On 2000 July 14 near 10:10 UT, a large solar flare with X-ray importance of X5.7 occurred near disk center in the NOAA active region (AR) 9077. The event comprised a 3B flare, eruption of a giant twisted filament, an extended Earth-directed coronal mass ejection (CME), and a large enhancement of accelerated particle flux in the corona and interplanetary space. This well-observed flare is often called the " Bastille Day 2000 " flare. The *Yohkoh* satellite observed an early phase (∼10:11–10:13 UT) and some of the impulsive phase (from ∼10:19:40 UT) of this flare classified as a long duration event (LDE). The soft X-ray telescope (SXT; Tsuneta et al. 1991) observed a large arcade. The width and length of the arcade were ∼30,000 and ∼120,000 km, respectively. The hard X-ray telescope (HXT; Kosugi et al. 1991) clearly showed a two-ribbon structure that corresponds to a series of footpoints of the soft X-ray (SXR) arcade.

Flares often exhibit a two-ribbon structure in the chromosphere, observed for example in Hα, and this pattern becomes especially pronounced for LDEs often associated with CMEs. In the Bastille Day flare, two ribbons were well seen in Hα (Yan et al. 2001). Fletcher & Hudson (2001) describe the morphology of the EUV ribbons, as seen in *Transiton Region and Coronal Explorer* (*TRACE*) data. The two-ribbon structure, however, had never been observed so clearly in hard X-rays (HXRs) until Masuda, Kosugi, &

Hudson (2001) analyzed the motions of bright HXR kernels (compact intense sources) in the two ribbons of the Bastille Day flare during the first and second bursts (S1 and S2) of emission in the HXT bands M1, M2, and H: 23–33, 33–53, and 53–93 keV, respectively. Even without accurate overlay of the HXR images of the flare on the photospheric magnetograms, Masuda et al. speculated that " these bright kernels are footpoints of newly reconnected loops " and that " lower loops, reconnecting early, are highly sheared; the higher loops, reconnecting later, are less sheared."

This key supposition supports the idea of three-dimensional reconnection in the corona at a separator with a longitudinal magnetic field. The idea being introduced to explain two subclasses of impulsive flares that have double footpoint HXR sources with increasing (decreasing) separation (Sakao, Kosugi, & Masuda 1997) is as follows. Suppose that two reconnecting field lines f_1 and f_2 pass through the separator, the second after the first (see Somov, Kosugi, & Sakao 1998, Fig. 4). If the first line f_1 has a stronger (weaker) longitudinal field than the second one, then the length of the line f_2 in the corona after reconnection becomes shorter (longer) than the length of the line f_1. Therefore, the distance between bright HXR footpoints in the chromosphere also becomes shorter (longer) as shown in Figure 5b in Somov et al. (1998). Such an obvious scenario is generally consistent with the observed motions of the HXR kernels in the Bastille Day flare. However, to make a judgement, we need to investigate relationship between the HXR kernels (their positions and dynamics) and the photospheric magnetic field (its structure and evolution).

With the aim of finding such relations, we adopt the following procedure. First, we overlay the HXR images of the

[1] Visiting professor from Astronomical Institute, Moscow State University, Universitetskij prospekt 13, Moscow 119992, Russia.

flare on the magnetograms by the Michelson Doppler Imager (MDI; Scherrer, Bogart, & Bush 1995) on board *SOHO*. Second, we overlay the obtained results of the first step on the magnetograms of high quality (Liu & Zhang 2001) obtained with the Solar Magnetic Field Telescope (SMFT) at Huairou Solar Observing Station (HSOS). The successful coalignment of the HXT images with the MDI and SMFT data allows us (1) to identify the most important MDI sunspots with the SMFT spots, whose morphology and evolution have been carefully studied and (2) to examine the relationships between the HXR kernel behavior during the impulsive phase of the flare and the large-scale displacements of the most important sunspots during two days before the flare. We describe our findings in § 2 and give their interpretation in § 3.

2. MAIN OBSERVATIONAL PROPERTIES

2.1. *Overlay HXR Images on Magnetograms*

To study the relationship between the HXR ribbons (especially kernels) and the underlying magnetic field, we must accurately coalign the *Yohkoh*/HXT data with simultaneous magnetic field data, first of all, the magnetograms from the MDI instrument on *SOHO*. In principle, such coalignment is possible using the pointing information of the two instruments. In practice, however, there are always errors in the pointing of different satellites and even different instruments on a single satellite. This makes the coalignment problem nontrivial. Concerning the Bastille Day flare, as observed by *SOHO* and *TRACE*, the best seems to be done by Fletcher & Hudson (2001). They have determined

the coalignment of data via cross-correlation of an image made in the white-light channel of *TRACE* with an MDI continuum image of NOAA AR 9077 taken at approximately the same time. This has allowed the authors to locate the EUV ribbon positions on the photospheric field to within ~2″. Then, under the assumption that the HXT pointing is reliable (see Fletcher & Hudson), the HXT and MDI images have been coaligned. When this has been done, the strongest HXR M2 sources occur at the same locations as the strongest EUV sources. This is reasonable from the physical point of view.

Figure 1 shows the HXR image synthesized during the peak of the flare at 10:27:00–10:27:20 UT; the blue contours are at 25%, 50%, 75%, and 90% of the maximum HXR intensity. The image is superposed by Fletcher & Hudson on the MDI magnetogram taken at 11:12 UT. White indicates a positive line-of-sight field, and black negative; the contours are at ±100, 500, and 1000 G. The broken straight line indicates the "simplified neutral line" (SNL) of the photospheric field, as introduced by Masuda et al. (2001). This line does not coincide with an actual photospheric neutral line (PNL) but is used as positional reference to describe dynamic behavior of the HXR sources.

We have added to this overlay notations of individual sunspots according to Liu & Zhang (2001). They describe the spots on the photospheric vector magnetograms obtained with the SMFT by the polarities with "P" and "F" representing the preceding and following polarities, respectively. There is a good spatial correspondence between spots as seen in the MDI magnetogram and spots in the magnetogram obtained with the SMFT at 08:43 UT with allowance for solar rotation. This allows us to identify
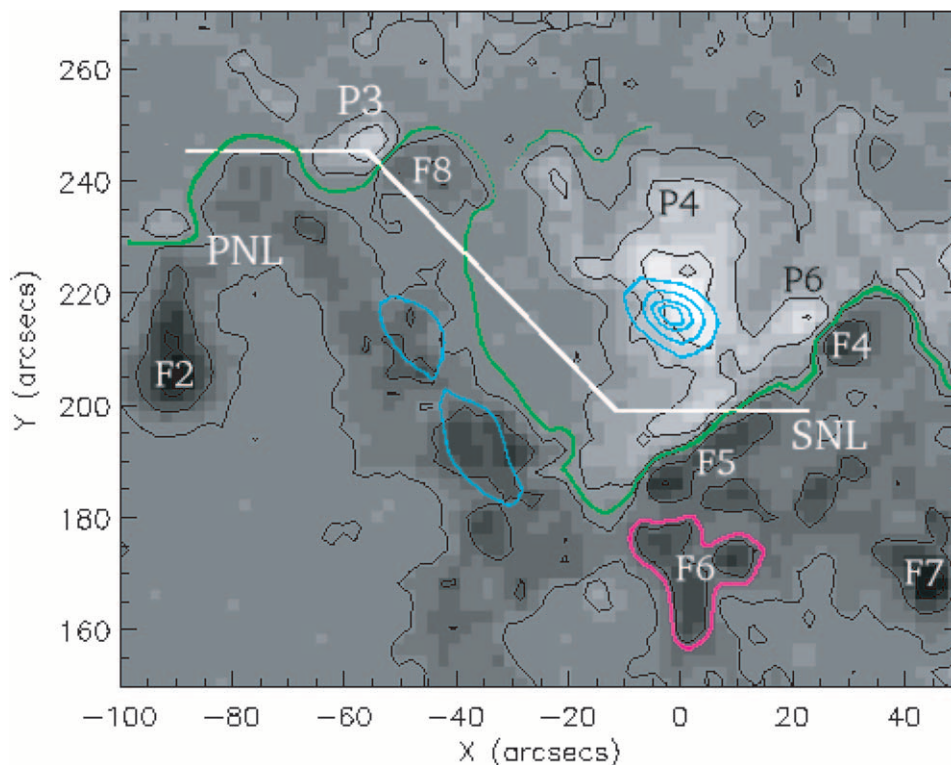

Fig. 1.—HXR source contours (*blue curves*) at the HXR maximum of the Bastille day flare overlaid on the MDI magnetogram. The green curve PNL represents the photospheric neutral line. SNL is the simplified neutral line.
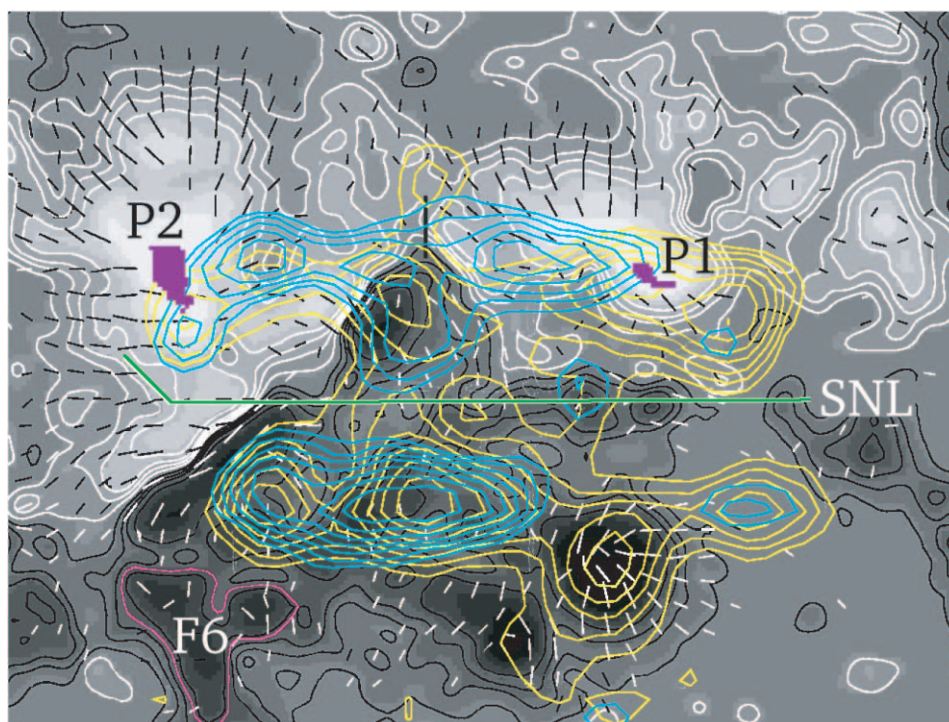
FIG. 2.—HXR source positions in the beginning of the first HXR spike S1 (*yellow contours*) and near its end (*blue contours*). The contour levels are 70.7, 50.0, 35.4, 25.0, 17.7, 12.5, and 8.8 of the peak intensity.

MDI spots with the corresponding spots in the SMFT magnetograms. For example, the "triangular" spot F6 in the MDI magnetogram in Figure 1 is the same to spot F6 in the SMFT magnetogram in Figure 2, in which an SMFT magnetogram taken at 08:43 UT on July 14, is shown from Figure 8*d* in Liu & Zhang (2001). The contour levels of the line-of-sight field are 160, 424, 677, and 1071 G. White contours represent positive polarity and black represent negative. The bars are transverse components with their length proportional to intensity. P1 and P2 are the most important positive sunspots.

To overlay the HXT data on the SMFT magnetogram we have used the pointing information for the satellite and HXT. This procedure gave us the relative position of the images taken in the same energy band during the different HXR spikes: S2 and S1, i.e., with a small difference in time. Since we already have the coalignment of the HXT data during the spike S2 and the magnetogram shown in Figure 1, we find the HXR source positions during the spike S1 at 10:19–10:24 UT on the SMFT magnetogram. Two *H*-band images during the spike S1, one in its rising phase and the other in decay phase, are overlaid in Figure 2. One, shown by yellow contours, is reconstructed in the beginning of the spike S1 at 10:19:37–10:20:27 UT. The second, shown by blue contours, is synthesized just after a peak (at about 10:22 UT) of the spike, at 10:22:17–10:22:45 UT. In this way, Figure 2 allows us to study the evolution of the HXR sources during the first spike. This will be done in the next section.

Some comments should be made here. First, the two-ribbon structure is quite clearly seen during the first spike. Moreover, the bright compact kernels in HXR are observed along the ribbons separated by the SNL in Figure 2. The appearance of the HXR kernels is not a surprisingly unex-

pectable result. The chromospheric Hα ribbons typically demonstrate several bright kernels. However, the intensity range of HXT was not high enough to observe the HXR ribbons in many flares as a typical phenomenon.

Second, if the whole system, i.e., the HXR ribbons and kernels together with the ridge of the huge arcade (Masuda et al. 2001, Fig. 5), is illuminated by fast electrons, then they must be accelerated in or above a large-scale system of magnetic loops. If we accept the standard two-dimensional MHD model of the two-ribbon flares, which is known as successful in interpretation of the *Yohkoh* SXT observations (Forbes & Acton 1996; Tsuneta et al. 1997), then this result is consistent with the hypothesis of a large-scale reconnection in the corona (see review by Aschwanden 2002). Moreover, because of the large scale and large energetics of the system of interacting magnetic fluxes, the reconnected parts of fluxes must be also large. Therefore, the problem of identification and measurement of the reconnected fluxes becomes essential (Fletcher & Hudson 2001).

2.2. *Motion of the HXR Kernels*

To see the strongest sources of HXR during the spike S1, we show in Figure 3 only the contours with levels 70.7%, 50.0%, 35.4%, and 25.0 % of the peak intensity. Two HXR ribbons are still well distinguished as two chains of the HXR kernels on either side of the SNL. The most intense kernel K2 in the southern ribbon shifts its position to the east with time. Its displacement is much slower, however, in comparison with that of the brightest kernel K1 in the northern ribbon. The displacement of the kernel K1 is shown by a green arrow. The source K1 moves to the north, i.e., outward from the SNL, and to a larger extent moves to the east, parallel to the SNL.
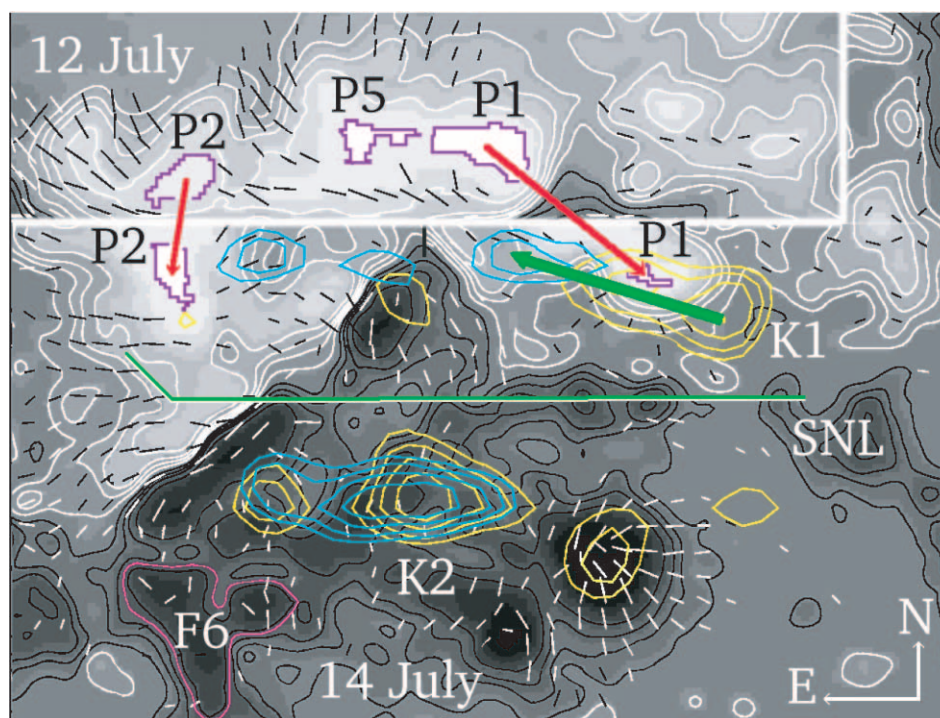
FIG. 3.—Position and motion of the strongest HXR sources K1 and K2 relative to the SMFT magnetogram on July 14

We will show that the observed displacement of the kernel K1 during the spike S1 can be related to the magnetic field evolution before the flare. It is reasonable to assume that some relationships between the HXR kernel motion and magnetic field structure and evolution do exist (Somov et al. 1998). However, it has not been known how these relations manifest themselves in actual flares or at least in theoretical models that are more realistic than the standard model (see discussion in Fletcher & Hudson 2001).

2.3. *Magnetic Field Evolution*

AR 9077 had one of the most complex field structures, a typical $\beta\gamma\delta$ class (Liu & Zhang 2001). It produced nearly 130 flares, including three flares of the X-class, the largest of those being the X5.7 flare on July 14. The next one in terms of X-ray importance was the X1.9 flare on July 12. We assume that just after this latter flare the AR had some minimum of magnetic energy and that 2 days were necessary for the AR to accumulate an energy sufficient for the Bastille Day flare. Generally, the sunspot motions cause the footpoints of magnetic fluxes to move and interact between themselves in the chromosphere and corona. In the absence of reconnection this process increases the nonpotential part of the magnetic energy, the excess available for the next flare. When the original (on July 12) configuration is deformed, magnetic gradients and stresses become enhanced. Moreover, slowly reconnecting current layers (RCLs) are created, and fast reconnection would be able to release the free magnetic energy as a flare.

Liu & Zhang (2001) have described the morphology of AR 9077, the proper motions of spots, and the evolution of the AR's magnetic fields. They have found many interesting peculiarities of the sunspot motions, including a suggested trigger of the flare, etc. However, the construction of an accurate model for such a complex group seems to be a difficult task. Instead we try a simpler task by restricting ourselves to large scales related to the HXR structure of the flare. Let us compare two magnetograms from a time sequence of magnetograms presented in Figure 8 in Liu & Zhang (2001). We overlay the magnetogram on July 12 in the top panel in our Figure 3 on the magnetogram on July 14 in the bottom panel. We see that the largest positive spot P1 rapidly moves southwest as shown by a long red arrow. Other big umbrae seem more stable or, at least, do not move so quickly as P1. This is seen from comparison with the displacement of the second positive spot P2 shown by the short red arrow.

Detailed descriptions of the proper motions are given by Liu & Zhang (2001). For example, a small part P5 (shown in our Fig. 3) of the umbra P1 moved away from the east end of P1 on July 12, but P5 still followed P1 as its east end on July 14. P1 became smaller, but tiny satellite spots formed around it. The small spots P5 and others moved in the same direction as one group. So, the southwestward motion of the large spot P1 together with its group is certainly one of the dominant motions in the AR. Other motions and changes of the magnetic field are presented in Liu & Zhang (2001), but they are presumably more important for the HXR spike S2. In this paper, we shall discuss only the first spike S1.

2.4. *HXR Kernels and Field Evolution*

The observed displacement of the brightest kernel K1 during the spike S1 is shown by the long green arrow in Figure 3, directed nearly antiparallel to the displacement of the spot P1 during two days between the two largest flares. An interpretation of this fact will be given in the next section. Here let us consider the observations in more detail, as
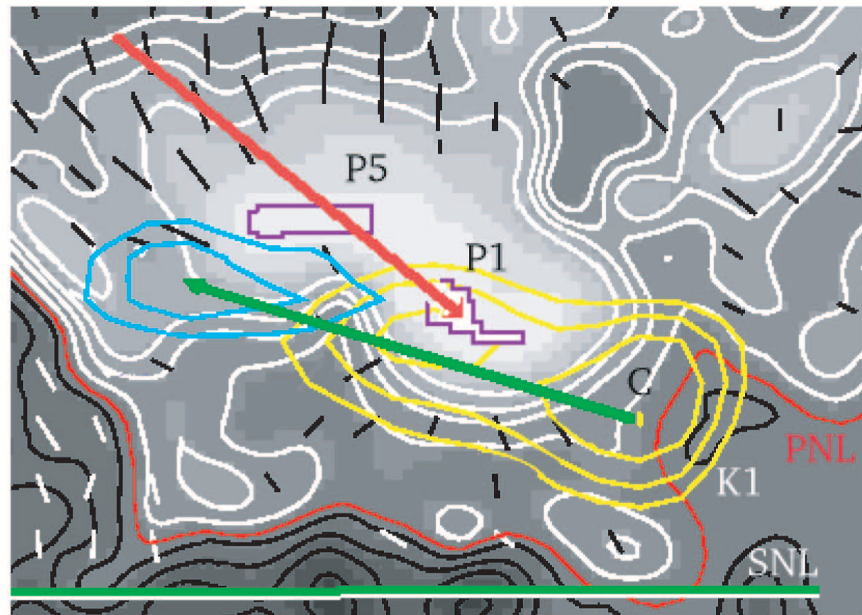
Fig. 4.—*H*-band images of the brightest kernel K1 in the rise and decay of the first HXR spike S1 overlaid on the SMFT magnetogram on July 14

shown in Figure 4 with the same contour levels as in Figure 3. In the rising phase of the spike, the kernel K1 appears in front of the moving spot P1, in its vicinity but not in the umbra. The brightest part of the kernel, the compact source indicated as the yellow point C in the beginning of the green arrow, is located in a region of weak line-of-sight field: between the contour of the 160 G and the actual neutral line, the red curve PNL in Figure 4.

This seems to be consistent with recent observations of several flares in the Hα line by a fast CCD camera installed at Big Bear Solar Observatory. Wang & Qiu (2002) compared the initial brightening of flare kernels at Hα-1.3 Å with photospheric magnetograms and found that initial brightenings avoided strong field regions. The observed Hα flare morphology and evolution suggest that the emission near a neutral line may originate from footpoints of flare loops of small height, where accelerated electrons precipitate first.

Figure 4 shows that the centroid of the most intense HXR source moves mostly antiparallel to the spot P1 displacement arrow but avoids the strongest field area. In the decay phase of the spike, the centroid arrives at the end of the green arrow in the vicinity of the spot P5 but still remains outside of the field level 1071 G. One of the possible reasons for such behavior might be in the magnetic-mirror effect (e.g., Somov & Kosugi 1997). Further investigation is necessary to understand the actual conditions of propagation, trapping, and precipitation of accelerated electrons from the corona into the chromosphere. However, the main problem in the flare physics still remains the primary release of energy, the transformation of the excess magnetic energy into kinetic energy of particles. Such transformation can be done by the collisionless reconnection at the separator with a longitudinal magnetic field. On the basis of the observational facts presented above, we are interested in understanding how such a mechanism could work in the Bastille Day flare.

3. THEORETICAL INTERPRETATION

3.1. *Classical Two-dimensional Reconnection Model as a Starting Point*

The two-dimensional reconnection models for solar flares, including the standard model, are definitely an over-simplification that cannot explain all features of actual flares. However, they have to be considered to find a missing element of the flare modeling and to demonstrate how this element should be introduced into the flare interpretation. Moreover, some features and predictions of the two-dimensional models still have to be studied and clarified. This concerns, first of all, the observational problem of identification and measurement of the reconnected fluxes in flares.

3.1.1. *Preflare Evolution and Energy Accumulation*

To recall notation, let us start from the classical two-dimensional reconnection in the plane (x, z) in Figure 5a. As usual, a two-dimensional model means that all the unknown functions do not depend of the coordinate y. In addition, we assume that there is no magnetic field component B_y. The straight line NL is the neutral line in the photospheric plane (x, y). Above the photospheric plane, six magnetic surfaces are shown to discuss the reconnection process. The magnetic surface 1 consists of the field lines that are similar to the line f_1 starting at the point a with coordinates $x = a$, $y = z = 0$. Surface 2 consists of the field lines similar to f_2.

Among the magnetic surfaces, two are topologically important: separatrices S_1 and S_2 cross at the separator straight line X. The separator separates the interacting magnetic fluxes by the separatrices. It is across the separator that the interacting fluxes are redistributed so that the field tends to keep a minimum energy. Figure 5a describes an "initial state" of the magnetic configuration in evolution. Starting from this state, let us introduce the converging flow of the photospheric footpoints. This is illustrated by Figure 5b by
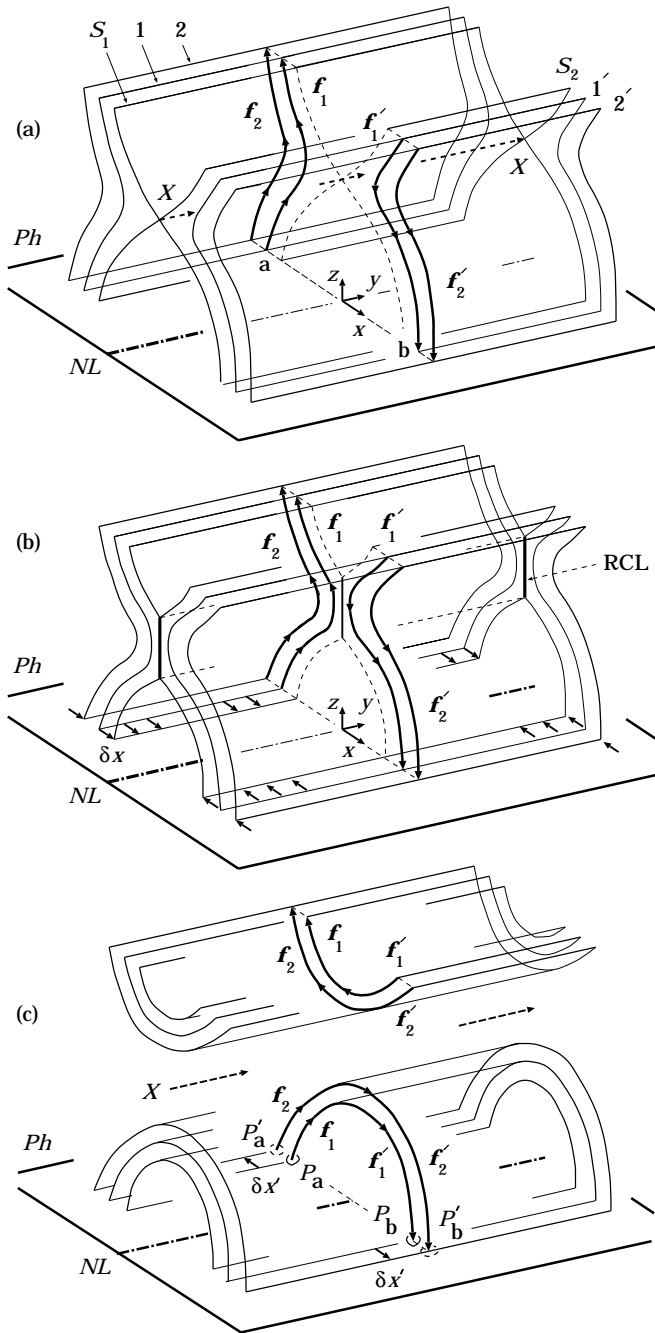
FIG. 5.—(*a*) An initial state of magnetic field. (*b*) The converging flows in the photosphere induce an RCL in the corona. (*c*) Apparent motion of footpoints during the fast reconnection process.

the displacement vector δx. We make the assumption that the reconnection process goes negligibly slowly, however. Some part of the magnetic fluxes would reconnect across the separator, if our assumption did not hold.

In a plasma of low resistivity, like coronal plasma, the slowly reconnecting current layer (see RCL in Fig. 5*b*) is developing and growing at the separator to hinder the redistribution of the interacting fluxes. This results in an excess energy being stored in the form of magnetic energy of an RCL. If J is the total electric current in the RCL and b is the half-width of the layer, then the surplus energy above that

of a potential field, having the same sources in the photosphere, is equal to (e.g., Somov 1992)

$$\mathscr{E}_f = \frac{1}{2c^2} L J^2 . \tag{1}$$

Here

$$L \approx 2l \ln \frac{2l}{b} \tag{2}$$

is the self-inductance of the RCL, l being its length along the separator, and c being the velocity of light.

In the case of the Bastille Day flare, the length of the arcade was $l \sim 10^{10}$ cm. With a typical RCL width $b \sim 10^9$ cm (see Somov 2000), we have $\ln(2l/b) \approx 3$ and

$$\mathscr{E}_f \approx \frac{3}{c^2} l J^2 \sim 3 \times 10^8 \, J(\mathrm{A})^2 \text{ ergs} . \tag{3}$$

Hence, the total current $J \sim 3 \times 10^{11}$–10^{12} A is necessary for a large flare, like the Bastille Day flare, to release the energy $\mathscr{E}_f \sim 3 \times 10^{31}$–$10^{32}$ ergs. This estimate does not contradict to the total current estimated from measurements of the magnetic field components in the photospheric plane in AR 9077 (Deng et al. 2001). A level of nonpotentiality in the AR (the total current, total current helicity and total energy) was higher before July 14 (see Fig. 5 in Deng et al. 2001) than after the flare and that predicted by equation (3). This presumably means that some part of magnetic energy is accumulated in surplus to the energy of the RCL, as an additional energy related to the photospheric shear (see §§ 3.3 and 3.4). On the other hand, during the Bastille Day flare, the total integrated thermal energy observed was $\lesssim 3 \times 10^{31}$ ergs (Aschwanden & Alexander 2001), which is smaller than the total energy of the flare predicted by equation (3). Therefore, a significant part of the flare energy might be converted directly into the kinetic energy of the fast plasma motions (i.e., CME) and accelerated particles.

3.1.2. *Flare Energy Release*

What is expected as a result of fast reconnection in the RCL during a flare? Figure 5*c* illustrates an expectation. Being in a high-temperature turbulent-current state (Somov 2000, chap. 17) the *rapidly* reconnecting layer provides powerful fluxes of energy along the reconnected field lines. The fluxes, when they arrive at the upper chromosphere, create an impulsive heating of the chromospheric plasma to high temperatures. Fast electrons (accelerated and superhot) lose their energy by collisions with thermal electrons of the chromospheric plasma. This creates a quick hydrodynamic and radiative response of the chromosphere (Somov 1992, chap. 2) observed in SXR, EUV, and optical emission. Inelastic collisions of the fast electrons with thermal protons generate the HXR bremsstrahlung radiation. Hence, the footpoints of the reconnected field lines also become bright in HXR.

We adopt the hypothesis that the flare ribbons observed by *TRACE* and *Yohkoh* in the Bastille Day flare map out the chromospheric footpoints of the field lines newly linked by reconnection (Aschwanden & Alexander 2001; Fletcher & Hudson 2001; Masuda et al. 2001). Since the field lines f_1 and f_1' reconnect first, they create the *first reconnected* line $f_1 f_1'$ and the first pair of chromospheric bright footpoints P_a and P_b as shown in Figure 5*c*. The field lines f_2 and f_2' will reconnect later on, for example at the end of the spike S1.

They will create a new pair of footpoints P'_a and P'_b in different locations. Obviously the distance between the footpoints will become larger with time. This is the well-known prediction of the standard model, explaining the well-observed effect of the increasing separation between flare ribbons.

The displacement $\delta x'$ represents the effect of fast relaxation of the nonpotential component of the field related to the RCL that has been generated by the photospheric converging flow. Note that, in general, $\delta x' \neq \delta x$. In the simplest example under consideration, the reason is obvious. Let the field lines f_1 and f'_1 coincide with the separatrices S_1 and S_2 of the initial state. Then δx represents a photospheric displacement of the initial separatrices, and the first bright footpoints P_a and P_b show the real displacement of the footpoints of the initial separatrices. This important feature of the two-dimensional reconnection models has to be taken into account when actual solar flares are considered. On the other hand, the apparent footpoint displacement $\delta x'$ is directed to the new positions of the bright kernels P'_a and P'_b. These are the footpoints of the separatrices in a final state of the field after reconnection. And the final state does not coincide with the initial one. It is natural to assume that $\delta x' \lesssim \delta x$ since dissipation of electric currents in solar flares is presumably never complete.

Therefore, the two-dimensional reconnection model predicts that the bright kernels, as they are seen in HXR, should separate in opposite directions from the PNL, if the photospheric magnetic fields converge to this line before a flare. However, actual flares are not so simple. Initially, on the basis of SXT observations, the flares with a "cusped arcade" (e.g., the 1992 February 21 flare) were considered as clear evidence in favor of the standard model (see Shibata et al. 1995, Tsuneta et al. 1997, and references therein). In a deeper examination of the SXT data, Uchida et al. (1998) and Morita et al. (2001) noted that there are some essential features inexplicable by the standard model. The apparent motion of the HXR kernels in the Bastille Day flare is one such feature, which will be discussed in the following sections.

3.2. Two-dimensional Reconnection with Longitudinal Magnetic Field

In the preceding section we neglected the component of the magnetic field parallel to the separator. Under actual conditions in the solar atmosphere, reconnection always occurs in the presence of a longitudinal component, however. The longitudinal component has several important physical consequences for the reconnection process. Only those that are important for understanding the apparent motions of chromospheric ribbons and kernels during a large two-ribbon flare will be discussed below.

We continue to assume that all the properties of the magnetic field are uniform in the y-direction, but now we allow the y-component of the field vector $\boldsymbol{B}$. Thus, the problem under consideration still remains a two-dimensional one (at least in the preflare evolution stage). Note that there is no reason to assume that the longitudinal component $B_\parallel = B_y$ is uniform in the plane (x, z); Somov et al. (1998) assumed that each field line arrives to the separator with its own value of $B_\parallel$.

Near the separator the longitudinal component $B_\parallel$ dominates because the orthogonal field $\boldsymbol{B}_\perp$ vanishes at the separator. Hence, the field lines passing close to the separator become elongated in the y-direction; the separator by itself is a unique field line. This and other properties of the separator are known since the work by Gorbachev et al. (1988); they will not be discussed here except for one of them. Reconnection in the RCL at the separator just conserves the flux of the longitudinal component (Somov 2000, chap. 17). The orthogonal components are reconnected and, therefore, participate in the connectivity change, but the longitudinal one does not. The longitudinal component plays a passive role in the topological aspect of the process, but it influences the reconnection rate (see Somov 2000).

So, in general, a three-component reconnection, i.e., the reconnection inside an RCL that has three components of magnetic field, at the separator can proceed with an increase (or decrease) of the longitudinal component of magnetic field and, as a consequence, with an increase (or decrease) of the length of the reconnected field lines. According to Somov et al. (1998), in the more impulsive flares, the reconnection process proceeds with a decrease of the longitudinal component and hence with a decrease of the footpoint separation.

3.3. Converging and Shear Flows and Three-dimensional Reconnection

Now we have reached a point where we can construct a scenario for the Bastille Day flare. Let us consider that, in addition to a converging flow, a shear flow is present in the photosphere (Fig. 6). When a field line, e.g., f_1, moves in direction to NL, it becomes longer along the NL under action of the shear flow. Figure 6a shows only those field lines that were initially in the plane (x, z), as shown in Figure 5a. Under action of the shear flow, they move out of the plane (x, z), except for an upper corona boundary, which is assumed, for the sake of simplicity, to be unaffected by the photospheric shear.

At the preflare evolution stage, the magnetic field sources in the photosphere have been displaced to their final preflare positions, but the plasma conductivity still can be considered as infinite, and the RCL prevents the interacting fluxes from reconnection. The energy of this interaction is just the energy of the magnetic field of the current layer, as discussed in § 3.1. Photospheric shear flows add to the energy of the prereconnection state the energy of magnetic tension generated by the shear because of the "freezing-in" property of the solar plasma. The photospheric flow works, making the field lines longer. This is always true, even if there is not a separator. In addition, if the magnetic field contains the separator, then the shear flows induce current layers extending along the separatrices, with the current flowing parallel to the orthogonal field $\boldsymbol{B}_\perp$ (Somov 2000, § 22.4).

From a mathematical point of view, if the magnetic force dominates all the others, the potential field is a solution of the MHD equations in the approximation of a strong field (Somov 2000, chap. 9). Such a field, changing in time according to the boundary conditions in the photosphere, sets the chromospheric and coronal plasma in motion. The field may remain mainly potential but accumulates the nonpotential components related to electric currents: (1) slowly reconnecting current layers, which are highly concentrated electric currents, flowing parallel to the separator and (2) smoothly distributed currents, which are responsible for magnetic tension generated by the photospheric shear flows.
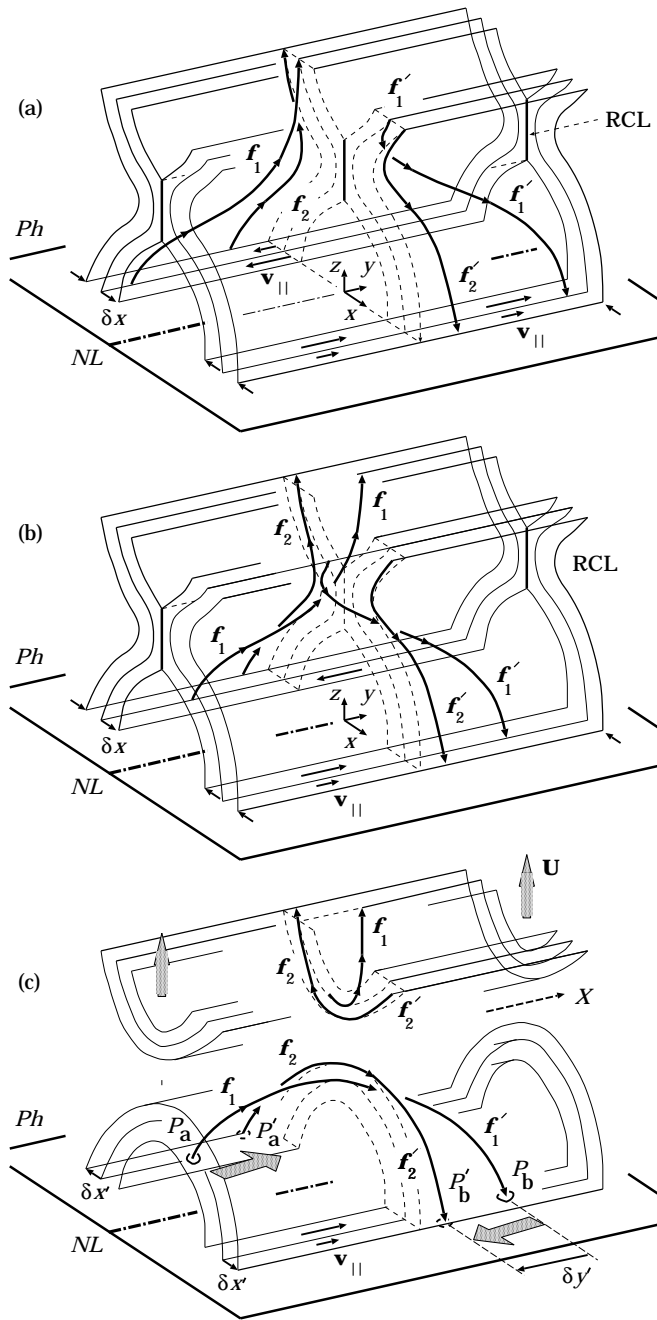
Fig. 6.—(*a*) Converging flows create the RCL. The shear flow in the photosphere makes the field lines longer. (*b*) A preflare state of the magnetic field in an AR. (*c*) Rapidly decreasing footpoint separation during a flare.

The fast reconnection stage of a flare, i.e., its impulsive phase, is illustrated by Figures 6*b* and 6*c*. As in the case of two-dimensional reconnection, only two pairs of the field lines are shown. Note, however, that Figure 6*b* differs from Figure 6*a* in one important respect. An additional assumption used here is that the physical conditions along the *y*-direction are not uniform any longer. The fastest reconnection place is assumed to be located in vicinity of the point $y = 0$ at the separator. For this reason, those field lines are delineated in Figure 6*b*, which have the nearest distance to the RCL at $y = 0$. Just these lines will reconnect first and quickly. Usually, in three-dimensional models, the place of

fast reconnection is chosen at the top of the separator, e.g., in a model for the flare of 1980 November 5 (Gorbachev & Somov 1990).

In this paper we do not consider the upward-moving reconnected field lines. They are indicated in Figure 6*c* by a velocity vector $\mathbf{U}$. As a consequence of the three-component reconnection at the separator, these lines take a twisted-flux-tube shape, which may correspond to a central helical part of a CME. On the other hand, the reconnected field lines below the separator shrink to form magnetic arcade loops. This part is discussed below.

Figure 6*b* shows only two pairs of the field lines that will reconnect at the point $y = 0$ in the RCL. Being reconnected, they create two pairs of the bright chromospheric footpoints shown in Figure 6*c*. The quickest release of energy creates, at first, the bright points P_a and P_b related to the *first* reconnected line $f_1 f_1'$. Later on, the field lines f_2 and f_2', being reconnected, create the field line $f_2 f_2'$ with the footpoints P_a' and P_b'. The apparent motion from P_a to P_a' and from P_b to P_b' now consists of two parts: $\delta x'$ and $\delta y'$. The first one has the same meaning as in the classical two-dimensional reconnection. The displacement $\delta y'$ is related to an increase of the length of the field lines, generated by the shear. Therefore, the displacement $\delta y'$ during the first HXR spike S1 in the Bastille Day flare represents the effect of relaxation of the nonpotential component of the field related to the photospheric shear.

Note that our model is just a central part of the so-called rainbow reconnection model (see § 4), which predicts the converging and shear flows in the photosphere under the top of the separator. Here the shear flow creates the longer magnetic loops, which, being reconnected first, provide the bright kernels with a large footpoint separation. Later on, the kernels with shorter separation appear. In this way, the more impulsive Sakao-type flares (see definitions of two sub-classes, more impulsive [MI] and less impulsive [LI] flares, in Sakao et al. 1997) with a decreasing footpoint separation can appear in AR.

We have proposed that, before a large two-ribbon flare with a decrease of footpoint separation, the separatrices are involved in a large-scale shear photospheric flow in the presence of an RCL generated by a large-scale converging flow. Other realizations of large flares are possible, of course, but this one seems to be the most plausible situation. In any case, the multiwavelength observations of the Bastille Day flare show that any scenario is incomplete unless it does not take into account the presence and eruption of a long twisted filament along the PNL before the flare (Liu & Zhang 2001; Yan et al. 2001). Bearing this morphological fact in mind, we are going to consider some physical processes near the PNL.

3.4. *Shear Flow and Photospheric Reconnection*

Let us return to Figure 6*a* and consider only the nearest vicinity of the NL. The width of the region that we are going to consider is $\lesssim 3 \times 10^8$ cm, much shorter than the typical distance between the separatrices of $\sim 3 \times 10^9$ cm. Thus, the separatrices are outside of the region under consideration. Note that the effects related directly to NL are dominant in this region. The converging flows toward the NL cause the opposite-polarity magnetic fields to collide in the photosphere and subsequently reconnect there. Converging flows in the photosphere have been reported from many observa-

tions (see Martin 1998). Moreover, flux cancellation has been frequently observed in association with the formation of a preflare filament prominence (e.g., Chae et al. 2001; Zhang et al. 2001).

Because of a shear flow, the footpoints on either side of the NL are displaced along it in opposite directions. This process produces a nonpotential structure, in which the projections of the field lines onto the photospheric plane *Ph* are more closely aligned with the NL. A motion toward the NL brings the footpoints closer together and further enhances the magnetic shear. Moreover, the converging flow makes the opposite-polarity fluxes interact and reconnect in the photosphere. The field lines arriving at the NL become disconnected from the photosphere to the prominence body. This leads to the formation of helical field lines which are capable, in principle, of supporting the prominence plasma (van Ballegooijen & Martens 1989).

The remarkable thing about photospheric reconnection is that reconnection effectively occurs only near the temperature minimum (Litvinenko & Somov 1994). Here the resistivity is especially high, and reconnection proceeds at a rate imposed by the horizontal converging flows. Magnetic energy is transformed into the thermal and kinetic energy of the resulting vertical motions. The upward flux of matter through the photospheric RCL into corona is capable of supplying 10^{17} g of weakly ionized plasma in a time of 10^5 s. This is amply sufficient for the formation of a huge prominence. In the preflare stage, the height h of such a filament prominence is presumably comparable with its width, so $h \lesssim 10^9$ cm (see Zhang et al. 2001, Fig. 1), and its gravitational energy

$$\mathscr{E}_g = mgh \lesssim 10^{17} \text{ g} \times (3 \times 10^4 \text{ cm s}^{-2}) \times 10^9 \text{ cm}$$
$$\sim 3 \times 10^{30} \text{ ergs} \qquad (4)$$

is large but still much smaller than the energy of a large flare $\mathscr{E}_{\text{fl}} \sim (1\text{–}3) \times 10^{32}$ ergs. Moreover, this mass requires an additional energy to accelerate it outward, as typically observed. Therefore, the flare energy has to be accumulated in other forms to push plasma upward (see Litvinenko & Somov 2001).

In the Bastille Day flare, the observations of *TRACE* in 171 and 195 Å together with the synchronous ground-based observations at HSOS showed that the filament rupture at some point at 09:48 UT seemed to activate the southwest part of the AR. At 10:10 UT a surge erupted, and a two-ribbon flare started to develop rapidly along the PNL (Liu & Zhang 2001). For this reason, we believe that the photospheric reconnection and filament eruption could somehow play a triggering role in this flare.

4. DISCUSSION AND CONCLUSIONS

Based on the preceding scenario and estimates, the Bastille Day flare energy was accumulated in the following forms:

1. Magnetic energy of the reconnecting current layer at the separator. This excess energy in the amount sufficient to produce a large flare is accumulated in the preflare AR in two days and can be quickly transformed into observed forms of the flare energy when the RCL becomes a high-temperature turbulent-current layer.

2. The magnetic energy of the current layers at the separatrices and the distributed currents generated in the AR by the photospheric shear flows, is sufficiently high to influence the reconnection process in the Bastille Day flare. In general, the energy of a large-scale ($\lesssim 10^9$ cm) sheared component of magnetic field may participate in energetics of the reconnection in the corona presumably with a positive (negative) contribution in more (less) impulsive Sakao-type flares.

In addition, in the vicinity of the photospheric neutral line, some part of energy is accumulated as the energy of a twisted filament. It is not clear, however, if we could consider this part of the preflare configuration in the force-free approximation, which would be the simplest model for a magnetic field to compute its surplus energy. The nonmagnetic forces, including the gas pressure gradient in a high-β plasma and the inertia-type term, in particular the centrifugal force (Shibasaki 2001), can make the non–force-free part locally significant in the preflare AR. Unfortunately, we do not know the value of the related energy excess either observationally or theoretically.

The non–force-free component participates in the flare development, but we do not know from observations whether it plays the primary role in a flare triggering or it is initiated somehow by reconnection in the corona (Uchida et al. 1998). For example, Antiochos, DeVore, & Klimchuk (1999) proposed that a coronal reconnection above a neutral line removes a magnetic flux that tends to hold down the sheared low-lying field and thereby allows the sheared field to erupt outward. *Yohkoh* and *SOHO* data do not seem to be capable of providing the necessary information to make a choice between these two possibilities. We hope this problem will be investigated with the upcoming *Solar-B* mission (Shimizu 1998).[2]

Reconnection at two levels, in the corona and at the photosphere, plays different roles. Photospheric reconnection seems to be mainly responsible for supply of a cold dense plasma upward, into preflare filament prominences. Coronal reconnection, being slow before a flare, allows the accumulation of a sufficient amount of magnetic energy. During a flare, the fast collisionless reconnection process in the corona, can convert this excess of energy into kinetic and thermal energies of fast particles and superhot plasma. As for the physical mechanism of the Bastille Day flare, we assume that it is the collisionless three-component reconnection at the separator in the corona (Somov et al. 1998).

Before a large-scale two-ribbon flare with an observed significant decrease of the footpoint separation, like the Bastille Day flare, two conditions are satisfied. First, the separatrices are involved in the large-scale shear photospheric flow, which can be traced by proper motions of main sunspots. The second condition is the presence of an RCL generated by large-scale converging motion of the same spots. These two conditions are sufficient ones for an AR to produce a huge two-ribbon flare. Other realizations of large flares are possible, of course, but this one seems to be the most plausible situation. Just this situation is predicted by the "rainbow reconnection" model (Somov 1986) illustrated by Figures 7 and 8.
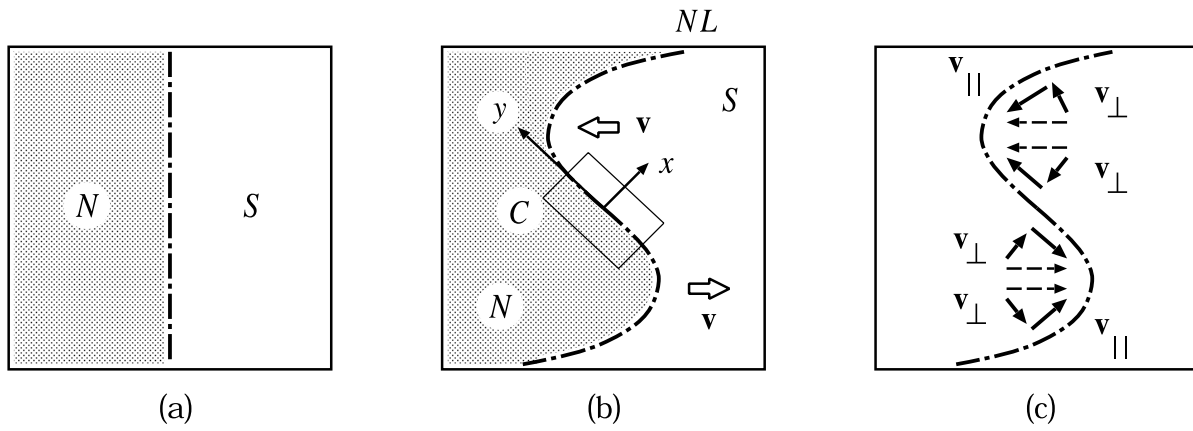

Fig. 7.—(a) Model distribution of magnetic field in the photospheric plane. (b) A photospheric vortex flow distorts the neutral line NL. (c) A schematic decomposition of the velocity field v into the components parallel and perpendicular to the NL.

Figure 7a shows the simplest model of the bipolar distribution of the vertical component B_z of the magnetic field in the photosphere. The neutral line divides the region into two zones. This region may be deformed by photospheric flows with the velocity field v in such a way that the neutral line gradually acquires the shape of the letter S as shown in Figure 7b. Beginning at a critical value of the curvature of the NL, the field calculated in the potential approximation begins to contain a separator, as shown in Figure 8. The separator X is located above the NL like a rainbow above a river that makes a bend. Note that the separator is nearly parallel to the NL in its central part.

Gorbachev & Somov (1988) showed this "rainbow reconnection" model reveals a causal connection of large two-ribbon flares with the S-shaped bend of the NL. The neutral line bending leads to appearance of the separator above the photosphere, and the necessary condition for reconnection in the solar atmosphere becomes satisfied. The model explains the arrangement and shape of the flare ribbons in the chromosphere, the early appearance of bright flare kernels, and the structure observed in SXR like two intersecting loops in the corona. These characteristic fea-

tures were explained, at first, in the well-observed homologous flares of 1980 November 5 (Gorbachev & Somov 1989, 1990).

Let us consider another consequence of the rainbow reconnection model. Figure 7c shows that the vortex-type flow generates two components of the velocity field; the velocity components $v_\parallel$ and $v_\perp$ are parallel and perpendicular to the photospheric NL. The first component provides a shear of field lines above the NL. The second one tends to drive reconnection in the corona (§ 3.1) and in the photosphere (§ 3.4). The effects of both velocity components are considered together in § 3.3. To demonstrate the basic physics in the simplest way, we considered only a central region C in the vicinity of the S-shaped neutral line NL in Figure 7b. Here we put the y-direction along the NL; the separator is nearly parallel to NL as was shown in Figure 5. In actual flares this "central part" can be long enough to be considered in this way. The Bastille Day flare seems to be a good example of such flares because of its extremely regular appearance as a beautifully "cylindrical arcade" in EUV and SXR (see illustrations in Aschwanden & Alexander 2001), which extends more than 10^{10} cm.
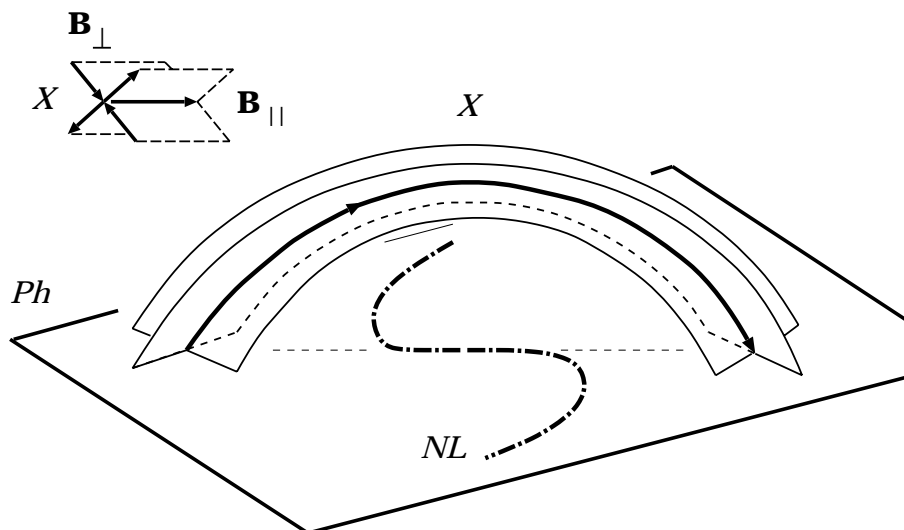

Fig. 8.—Separator X above the S-shaped bend of the photospheric neutral line NL according to Somov (1985)

During the Bastille Day flare, two excesses of magnetic energy are released completely or partially. Our model describes the first HXR spike and the western half of the flare. The model explains two kinds of apparent motions of the HXR kernels. An increase of a distance between the flare ribbons in which the HXR kernels appear results from fast magnetic reconnection in a coronal current layer. The second effect is a decrease of the distance between the kernels quickly moving to each other as a result of relaxation of magnetic tensions generated by the photospheric shear flows. Both features are typical for the more impulsive Sakao-type flares.

REFERENCES

Antiochos, S. K., DeVore, C. R., & Klimchuk, J. A. 1999, ApJ, 510, 485
Aschwanden, M. J. 2002, Space Sci. Rev., in press
Aschwanden, M. J., & Alexander, D. 2001, Sol. Phys., 204, 93
Chae, J., Wang, H., Qiu, J., Goode, P. R., Strous, L., & Yun, H. S. 2001, ApJ, 560, 476
Deng, Y., Wang, J., Yan, Y., & Zhang, J. 2001, Sol. Phys., 204, 13
Fletcher, L., & Hudson, H. 2001, Sol. Phys., 204, 71
Forbes, T. G., & Acton, L. W. 1996, ApJ, 459, 330
Gorbachev, V. S., Kelner, S. R., Somov, B. V., & Shwarz, A. S. 1988, Soviet Astron., 32, 308
Gorbachev, V. S., & Somov, B. V. 1988, Sol. Phys., 117, 77
———. 1989, Soviet Astron., 33, 57
———. 1990, Adv. Space Res., 117, 77
Kosugi, T., et al. 1991, Sol. Phys., 136, 17
Litvinenko, Yu. E., & Somov, B. V. 1994, Sol. Phys., 151, 265
———. 2001, Space Sci. Rev., 95, 67
Liu, Y., & Zhang, H. 2001, A&A, 372, 1019
Martin, S. F. 1998, Sol. Phys., 182, 107
Masuda, S., Kosugi, T., & Hudson, H. S. 2001, Sol. Phys., 204, 55
Morita, S., Uchida, Y., Hirose, S., Uemura, S., & Yamaguchi, T. 2001, Sol. Phys., 200, 137
Sakao, T., Kosugi, T., & Masuda, S. 1997, Observational Plasma Astrophysics: Five Years of Yohkoh and Beyond, ed. T. Watanabe, T. Kosugi, & A. Sterling (Dordrecht: Kluwer), 273

Scherrer, P. H., Bogart, R. S., Bush, R. I., et al. 1995, Sol. Phys., 162, 129
Shibasaki, K. 2001, ApJ, 557, 326
Shibata, K., Masuda, S., Shimojo, M., Hara, H., Yokoyama, T., Tsuneta, S., Kosugi, T., & Ogawara, Y. 1995, ApJ, 451, L83
Shimizu, T. 1998, Crossroads for European Solar and Heliospheric Physics, ed. E. R. Priest, F. Moreno-Insertis, & R. A. Harris (ESA SP-417; Noordwijk: ESA), 169
Somov, B. V. 1985, Soviet Phys.—Uspekhi, 28, 271
———. 1986, A&A, 163, 210
———. 1992, Physical Processes in Solar Flares (Dordrecht: Kluwer)
———. 2000, Cosmic Plasma Physics (Dordrecht: Kluwer)
Somov, B. V., & Kosugi, T. 1997, ApJ, 485, 859
Somov, B. V., Kosugi, T., & Sakao, T. 1998, ApJ, 497, 943
Tsuneta, S., Masuda, S., Kosugi, T., & Sato, J. 1997, ApJ, 478, 787
Tsuneta, S., et al. 1991, Sol. Phys., 136, 37
Uchida, Y., et al. 1998, Ap&SS, 264, 145
van Ballegooijen, A. A., & Martens, P. C. H. 1989, ApJ, 343, 971
Wang, H., & Qiu, J. 2002, ApJ, 568, 408
Yan, Y., Deng, Y., Karlicky, M., Fu, Q., Wang, S., & Liu, Y. 2001, ApJ, 551, L115
Zhang, J., Wang, J., Deng, Y., & Wu, D. 2001, ApJ, 548, L99